IOSR Journal of Computer Engineering (IOSR-JCE)
e-ISSN: 2278-0661,p-ISSN: 2278-8727
PP 58-60
www.iosrjournals.org

Childhood Bone Marrow And Artificial Neural Network

Dr. V. Uma Rani,Assistant , Professor B.Ramya , Research Scholar
1.Department of Computer Science,Sri Ramakrishna College of Arts and Science for Women,Coimbatore, India
2.Department of Computer Science, Sri Ramakrishna College of Arts and Science for Women,,Coimbatore,,India

Abstract: *Childhood leukemia, the most common type of cancer in children and teens, is a cancer of the white blood cells. Abnormal white blood cells form in the bone marrow. They quickly travel through the bloodstream and crowd out healthy cells. This raises the body's chances of infection and other problems. One of the Machine Learning Algorithm Artificial Neural Network is used to find the leukemia, An artificial neural network is an interconnected group of nodes, akin to the vast network of neurons in a brain.. For data regression and prediction, Visual Gene Developer's NeuralNet class is used*

Keywords: *Childhood leukemia, Machine Learning , artificial neural network, NeuralNet White blood cells.*

I. Introduction

The bone marrow is a soft, spongy tissue found inside the bones. The bone marrow in the hips, breast bone, spine, ribs, and skull contains cells that make the body's blood cells. The bone marrow is responsible for the development and storage of most of the body's blood cells. The three main types of blood cells made in the bone marrow include. Red blood cells (erythrocytes). These cells carry oxygen to the tissues in the body. White blood cells (leukocytes). These cells help fight infections and aid in the immune system. Platelets. These help with blood clotting. Each of these cells carries a life-maintaining function. The bone marrow is a vital part of the human body. Childhood leukemia, the most common type of cancer in children and teens, is a cancer of the white blood cells. Abnormal white blood cells form in the bone marrow. They quickly travel through the bloodstream and crowd out healthy cells. This raises the body's chances of infection and other problems.

II. Artificial Neural Networks

ANNs are composed of multiple nodes, which imitate biological neurons of human brain. The neurons are connected by links and they interact with each other. The nodes can take input data and perform simple operations on the data. The result of these operations is passed to other neurons. The output at each node is called its activation or node value .Each link is associated with weight. ANNs are capable of learning, which takes place by altering weight values.

3.1Machine Learning in ANNs

ANNs are capable of learning and they need to be trained. There are several learning strategies :

- **Supervised Learning** − It involves a teacher that is scholar than the ANN itself. For example, the teacher feeds some example data about which the teacher already knows the answers. For example, pattern recognizing. The ANN comes up with guesses while recognizing. Then the teacher provides the ANN with the answers. The network then compares it guesses with the teacher's "correct" answers and makes adjustments according to errors.
- **Unsupervised Learning** − It is required when there is no example data set with known answers. For example, searching for a hidden pattern. In this case, clustering i.e. dividing a set of elements into groups according to some unknown pattern is carried out based on the existing data sets present.
- **Reinforcement Learning** − This strategy built on observation. The ANN makes a decision by observing its environment. If the observation is negative, the network adjusts its weights to be able to make a different required decision the next time.

3.2 Bayesian Networks

These are the graphical structures used to represent the probabilistic relationship among a set of random variables. Bayesian networks are also called **Belief Networks** or **Bayes Nets.** BNs reason about uncertain domain. There is an only constraint on the arcs in a BN that you cannot return to a node simply by following directed arcs. Hence the BNs are called Directed Acyclic Graphs (DAGs).

III. Indentations And Equation

4.1 DIRECTED ACYCLIC GRAPH

Each node in a directed acyclic graph represents a random variable. These variable may be discrete or continuous valued. These variables may correspond to the actual attribute given in the data. In this paper, a new image representation algorithm, "Projected Principal-Edge Distribution" (PPED), was used . The algorithm was developed for use in the image recognition system hardware based on the neural associative processors, and the computing speed can be greatly improved. The PPED algorithm was a type of feature recognition algorithm that is sensitive to edge shape, and the algorithm was simple to actualize. The PPED features were extracted from the WBC images, which were segmented by the method mentioned above. The resolution of the images of WBCs captured by the CMOS shadow imaging system was low. The PPED algorithm was demonstrated to be a useful method to sort the three subtypes of WBCs in this system. To verify the algorithm, the 20×, 10×, and 4× objective lenses of the microscope were used as a reference system to compare the proposed shadow imaging instrument. Therefore, the PPED algorithm could be used to extract the image feature vector, and then it could be used for WBCs classification.

4.2 WBC classification algorithm

A method to classify WBCs compared the distance between two feature vectors of the cells. The smaller the distance between the two feature vectors, the more likely the two cells were the same type. It was calculated using the Euclidean distance between two vectors.

Euclidean distance: $d(\mathrm{x},\mathrm{y}) = \left[\sum_{i=1}^{n}(x_i - y_i)^2\right]^{1/2}$

In this paper, the classification method that measured the distance between the PPED feature vector of each cell and the three subtypes of standard PPED feature vectors was used, and the standard PPED vector. The high-resolution images of the WBCs captured by the 10× objective lens were used to recognize three subtypes of leukocytes manually. The low-resolution images of WBCs captured by the 4× objective lens were used to extract the standard PPED vector. The low-resolution images of the WBCs could not be used to easily recognize the subtypes of WBCs manually, but the high-resolution images of the same cell could. Finally, the standard PPED vectors of the three subtypes were calculated by the PPED method mentioned in a previous paper, and the standard PPED feature.

The images of the WBCs captured by the CMOS shadow imaging system had low resolution, and other features should be added to improve the accuracy of the WBC classification. The size of the WBCs was a useful and important feature, which was close to the edge of the image and reduced the false recognition rate, providing a more accurate classification of the WBCs. The Euclidean distance of each cell to the standard vector was shown as $D_p(i) = \left[\sum_{m=0}^{63}(P_d(j) - V_m(j))^2\right]^{1/2}\ i \in \{Neu, Mon, Lym\}.$

Here, D_p was the Euclidean distance of the Ith cell PPED vector from the standard vector. The subscript m indicates the three subtypes of WBCs, neutrophil (Neu), monocyte (Mon) and lymphocyte (Lym). However, the low-resolution images lead to inaccurate classification of the WBCs. The missing details of the cell image, caused by low resolution, made the feature extraction of different types of cells difficult. Therefore, we propose a novel algorithm that normalizes the distance between PPED and the standard vector center and then converts the value to

$$D_m(i) = \frac{D_p(i)}{\operatorname{argmax}(D_p(i))}\ i \in \{Neu, Mon, Lym\},$$

probability:

$P_m(i) = 1 - D_m(i)\ i \in \{Neu, Mon, Lym\}.$

Here, $D_m(i)$ was the normalized Euclidean distance and the $P_m(i)$ was the probability of the three subtypes of WBCs. The largest, the median and the smallest sized WBCs were the neutrophil, monocyte and lymphocyte, respectively. By the size of the cell, it was preliminary to determine which types the cell belongs to, the method shown as

$$t = \begin{cases} Lym,\ 5\mu m < d < 10\mu m \\ Neu, 10\mu m < d < 14\mu m \\ Mon, 14\mu m < d < 25\mu m \end{cases}.$$

Here, t was the types of the WBCs and d was the diameter of the WBCs. Then, the probability Ps(i) distinguished by the size of WBCs was shown as

$$P_s(i) = \begin{cases} 1,\ i = t \\ 0,\ i \neq t \end{cases}\ i, t \in \{Neu, Mon, Lym\}. \quad \textbf{(13)}$$

This probability $P_m(i)$ accounts for 90% of the weight of the judgment, and the probability $P_s(i)$ accounts for 10%. The function of different types of WBC classifications was shown as $T_m(i) = 0.9 \times P_m(i) + 0.1 \times P_s(i) \;\; i \in \{Neu, Mon, Lym\}$, **(14)** where $T_m(i)$ was the probability of the three subtypes of WBCs. For every sample, three $T_m(i)$ values could be calculated, which show neutrophils, monocytes and lymphocytes. Which $T_m(i)$ value was the largest, which corresponded to the type of cells.

IV. Figures And Tables

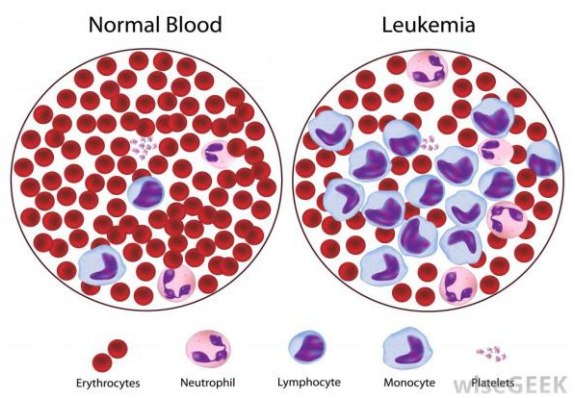

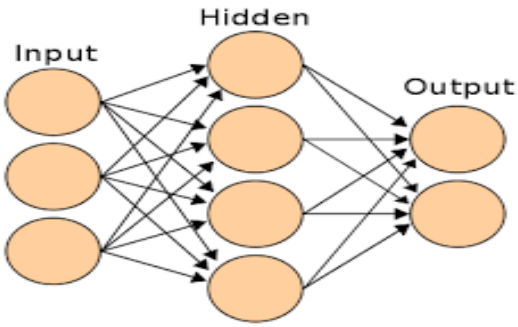

V. Conclusion

In summary, a WBC classification method based on shadow imaging of a CMOS sensor was proposed. The system contained inexpensive parts, such as the CMOS sensor, a white LED and an aluminum alloy shell, and the total cost of this system was below $100. A white LED was used in the proposed system, which means that the LED could be replaced by sunlight. The system power consumption would be significantly reduced and more conducive to POCT with sunlight. Due to the algorithms proposed in this paper, the system was not only cheaper but also automated. For the blood tests from whole blood samples from six outpatients (proportion of WBCs), the result obtained was a mean correlation index of 0.96. The mean errors of percentage of neutrophils (3.45%), monocytes (6.04%) and lymphocytes (6.7%) were lower than the method proposed by Mohendra Roy . Although the performance was still less than traditional methods, it was sufficient to demonstrate that the proposed instrument and classification method were effective. The instrument was 10 × 10 × 10 cm in volume, but the aluminum alloy shell could be further reduced to chip size. The widespread application of the instruments would provide a more convenient method of routine blood examination.

References

Journal Papers:

[1] Gwaiz L A: BONE MARROW NECROSIS. Annals of Saudi Medicine 1997; 17, No 3,374-376.
[2] Naguib R N G, Sherbet G V: artificial neural networks in cancer diagnosis: prognosis and patient management. CRC press 2001.
[3] SordoM : introduction to neural networks in health care. Open clinical knowledge management for medical care 2002; 1-17.
[4] Khonglah Y, Basu D and Dutta T K: Bone marrow trephine biopsy findings in chronic myeloid leukemia. Malaysian J Pathol 2002; 24(1), 37 – 43.
[5] Richard K: Use of an artificial neural network to quantitate risk of malignancy for abnormal mammograms. Surgery 2001; 459-466.
[6] Bhutani M, Kochupillai V and Bakhshi S: Childhood Acute Lymphoblastic Leukemia: Indian Experience. Indianjournalofmedical&paediatric oncology 2004; 25, Suppl. 2, 3-8.
[7] J.M. Garcia-Gomez, C. Vidal, J. Vicente, L. Marti-Bonmati and M. Robles, Medical decision support system for diagnosis of soft tissue tumors based on distributed architecture, 26th Annual International Conference of the IEEE EMBS (2004).
[8] D. Michie, D.J. Spiegelhalter and C.C. Tayor, Machine learning, neural and statistical classification, Ellis Horwood, London, 1994.
[9] J. Quinlan, Induction of decision trees, Machine Learning, Morgan Kaufmann 1986, 81–106. [19] S. Sahan, K. Polat, H. Kodaz and S. Gunes, A new hybrid ¨ method based on fuzzy-artificial immune system and k-nn algorithm for breast cancer diagnosis, Computers in Biology and Medicine 37 (2007), 415–423.
[10] I. Sefion, M. Gailhardou and A. Ennaji, A Medical Decision Support System for Asthmatic Patient Health Care, Artificial Intelligence and Applications (AIA) (2002), 362–344.